Bulletin of Electrical Engineering and Informatics
Vol. 15, No. 1, February 2026, pp. 290~301
ISSN: 2302-9285, DOI: 10.11591/eei.v15i1.10530

GNN data association based multi-target localization and vital signs monitoring using SIMO-UWB sensor network

Meraouli Hadjer Rania[1], Slimane Zohra[2], Abdelmalek Abdelhafid[2]
[1]Structures Intelligentes Laboratory (SSL), Department of Electronic and Telecommunication, Faculty of Science and Technology, Belhadj Bouchaib University, Ain Témouchent, Algeria
[2]STIC Labs, Department of Telecommunication, Faculty of Technology, Abou Bekr Belkaid University, Tlemcen, Algeria

Article Info

Article history:

Received Apr 18, 2025
Revised Oct 4, 2025
Accepted Dec 6, 2025

Keywords:

Impulse ultra-wideband
Multiple targets
Time of arrival
Trilateration
Vital signs

ABSTRACT

This paper presents a method for multi-target localization and vital signs monitoring using impulse ultra-wideband (UWB) technology. A single-input multiple-output (SIMO) sensor network is employed to enable simultaneous signal reception, which introduces challenges in signal separation and precise target positioning. The primary difficulty arises from the data association problem, where measurements must be correctly assigned to their respective targets, particularly in cases of overlapping signals or closely spaced targets. To address this issue, a time of arrival (TOA) algorithm is applied to estimate target ranges, while all possible measurement–target associations are evaluated. Subsequently, true target positions are obtained through trilateration combined with the global nearest neighbor (GNN) method. For vital signs monitoring, the continuous-time Fourier transform (CTFT) is utilized to estimate respiratory and cardiac rates. Experimental results demonstrate high accuracy, with relative errors of 1.42% in distance estimation, 2.34% in breathing rate, and 0.73% in heart rate estimation.

Corresponding Author:

Meraouli Hadjer Rania
Structures Intelligentes Laboratory (SSL), Department of Electronic and Telecommunication
Faculty of Science and Technology, Belhadj Bouchaib University
Ain Temouchent, Algeria
Email: hadjer.meraouli@univ-temouchent.edu.dz

1. INTRODUCTION

Vital signs, particularly respiratory and cardiac indicators, are critical for assessing an individual's physiological state and play a central role in diagnosis, monitoring, and clinical evaluation. They are applied in diverse healthcare domains, including asthma management, heart failure monitoring, neonatal care, and disaster response. Among the various technologies developed for vital sign monitoring, ultra-wideband (UWB) radar has emerged as a leading solution due to its high resolution, energy efficiency, and ability to capture subtle physiological movements. Nevertheless, most existing studies have primarily focused on single-subject monitoring [1], whereas practical applications such as patient surveillance in hospitals and victim detection in disaster scenarios demand the simultaneous monitoring of multiple individuals [1].

To address this requirement, different radar architectures have been investigated, single-input single-output (SISO) radar [2]–[4] offers simplicity but suffers from limited spatial diversity, making it difficult to distinguish multiple targets located at the same range. Single-input multiple-output (SIMO) radar [1], [5], [6] enhances spatial resolution by exploiting distributed antennas, while multiple-input multiple-output (MIMO) radar systems [7]–[9] provide improved target detection and parameter estimation through waveform diversity. In addition, non-radar modalities such as wireless fidelity (WiFi-based) sensing and camera-based surveillance have been explored as complementary solutions [10], [11]. Within this context,

two main approaches have been proposed for monitoring the vital signs of multiple subjects: one based on target direction information and the other on range information. The first solution uses angle of arrival (AoA) to separate targets [1], [6], [12]–[14]. To achieve this, several techniques have been developed such as mechanical scanning (MS) [12], phased array antenna (PAA) [13], metamaterial (MTM), leaky-wave antenna (LWA) [14], and digital beamforming [1], [6]. Most of these methods effectively separate multiple targets positioned at the same distance. The second approach focuses on separating the vital signs of individuals based on their different distances. Several approaches have been proposed for multi-target separation and vital sign monitoring [2], [9], [15]–[20]. Wavelet analysis (WA) [2] enables signal decomposition but may suffer from sensitivity to noise. Through-wall UWB-MIMO radar with stepped- frequency continuous-wave (SFCW) transmission [9], improves penetration and target detection, though at the cost of system complexity. Variational mode decomposition (VMD) [15] effectively separates respiration components from multiple subjects at the same distance, yet its performance degrades under strong interference. Modified cell-average constant false alarm rate (MCA-CFAR) based processing [16] enhances detection accuracy, but remains limited by parameter tuning in cluttered environments. UWB-MIMO with iterative adaptive approach (IAA) [17] achieves low side lobes and improved separation, albeit with higher computational load. Fast Fourier transform (FFT) with variance statistics [18], and cross-correlation [19] provide simpler alternatives for multi-subject detection, but both struggle to reliably distinguish vital signs of individuals located at the same distance.

To overcome the limitation of time of arrival (TOA) in distinguishing multiple targets located at the same distance, we propose a SIMO-based methodology that employs three single-antenna sensors, where one operates as a transceiver and the other two serve as receivers. This configuration facilitates spatial diversity by capturing multiple copies of the transmitted signal at distinct spatial locations. By analyzing the differences in TOA across these receivers, trilateration techniques is applied to precisely estimate the distance and spatial coordinates of each target. Such spatial information enables the effective separation of targets even when they are positioned at similar ranges. Subsequently, the continuous-time Fourier transform (CTFT) is performed to accurately estimate the respiratory rate and heart rate of each target.

The rest of this paper is structured as follows: section 2 introduces the mathematical model for vital signs. Section 3 presents the proposed monitoring method for estimating the position and vital sign rates of each target. Section 4 discusses the experimental results, while section 5 concludes the study.

2. VITAL SIGNS MODEL

UWB impulse radar has been extensively² employed for vital signs detection due to its high resolution. The cyclical contraction and expansion of the chest cavity, induced by respiratory and cardiac activities, generate periodic motions resembling sinusoidal waveforms. These motions cause minute displacements in the chest position, typically on the order of a few millimeters. Such displacements result in measurable phase variations in the radar's received signal, thereby facilitating accurate monitoring and assessment of vital signs.

In our approach, a SIMO sensor network is employed, comprising one active sensor operating in a bistatic mode (simultaneously transmitting and receiving) and multiple passive sensors functioning solely as receivers. Assuming K target, the channel response can be expressed as (1):

$$h(t,\tau) = \sum_{k=1}^{K} \alpha^k \, \delta\big(\tau - \tau^k(t)\big) + \sum_i \alpha_i \delta(\tau - \tau_i) \quad (1)$$

$\alpha^k \delta\big(\tau - \tau^k(t)\big)$ represents the time-varying components associated with human vital signs, caused by the periodic chest movements due to respiration and heartbeat, $\sum_i \alpha_i \delta(\tau - \tau_i)$ denotes the static clutter response.

The received signal in the fast time domain can be represented as the convolution of the transmitted UWB the channel response, the received signal at the active antenna can be formulated as (2) [1], [21]:

$$r(t,\tau) = g(\tau) * h(t,\tau) = \sum_{k=1}^{K} \alpha^k \, g\big(\tau - \tau^k(t)\big) + \sum_i \alpha_i g(\tau - \tau_i) \quad (2)$$

Conversely, the signal received at the passive sensors consists of the target echoes combined with the pulse transmitted by the active antenna and can be expressed as (3):

$$\tilde{r}(t,\tau) = \sum_{k=1}^{K} \alpha^k \, g\big(\tau - \tau^k(t)\big) + g(\tau) + \sum_i \alpha_i g(\tau - \tau_i) \quad (3)$$

Where: τ and t indicate respectively the fast time and slow time, c is speed of light, and $g(\tau)$ is the transmitted pulse, α^k and τ^k denote the attenuations and the TOA corresponding to the k^{th} person, respectively, and $x(t,\tau)$ is measurement noise.

Considering that the human chest remains stationary during the coherent processing interval, the TOA of the signal received by the active sensor can be expressed as (4) [22]:

$$\tau^k(t) = \frac{2\,d_0^k}{c} + \frac{2\,d_b^k \sin\left(2\pi f_b^k t\right)}{c} + \frac{2\,d_h^k \sin\left(2\pi f_h^k t\right)}{c} \quad (4)$$

Conversely, the TOA of the signal received by the passive sensors can be expressed as (5):

$$\tau_r^k(t) = \frac{d_0^k + d_r^k}{c} + \frac{2\,d_b^k \sin\left(2\pi f_b^k t\right)}{c} + \frac{2\,d_h^k \sin\left(2\pi f_h^k t\right)}{c} \quad (5)$$

Where: d_0^k represents the mean distance between the active sensor and target k, d_r^k represents the mean distance between the passive sensor and target k, d_b^k, d_h^k represent the breathing and heartbeat displacement amplitudes corresponding to the k^{th} person, respectively, f_b^k, f_h^k represent the breathing and heartbeat frequencies corresponding to the k^{th} person, respectively.

3. PROPOSED MONITORING METHOD

This section presents a SIMO radar system operating at a center frequency of 6 GHz. The system consists of three sensor devices: one functioning in both transmission and reception modes, and two dedicated solely to reception. The setup is designed to determine the positions of multiple targets and includes a method for estimating vital sign rates based on the measured distances. Before presenting our proposed localization method, it is essential to address a fundamental challenge in multi-target systems, namely the problem of multiple-target measurement association.

3.1. Multiple targets measurements association

Data association is a fundamental step in multi-target tracking, aiming to correctly match sensor measurements to their corresponding targets. The task becomes particularly challenging when targets are closely spaced, leading to high ambiguity in distinguishing measurements. Several techniques have been developed to address this problem: nearest neighbor (NN) offers simplicity and low cost but often fails under high target density. Global nearest neighbor (GNN) improves accuracy through global optimization at the expense of higher complexity. Multiple hypothesis tracking (MHT) provides robust performance by maintaining parallel hypotheses, though it suffers from exponential growth in computation. Joint probabilistic data association (JPDA) assigns probabilistic weights to all feasible associations, balancing robustness and complexity [23].

3.2. Single-input multiple-output system

The proposed system is modeled and simulated in MATLAB/Simulink and is composed of three main components: sensors, the propagation channel, and the targets. The sensor subsystem includes a transmitter, multiple receivers, and a signal processing unit, as shown in Figure 1.

To separate multiple targets and monitor their vital signs, the system employs an array of three UWB sensors and utilizes the SIMO technique to effectively differentiate between multiple targets. The transmitter emits a sequence of UWB pulses centered at 6 GHz, within the Federal Communications Commission (FCC) UWB range of 3.1 GHz to 10.6 GHz, generated through signal processing algorithms. The choice of this central frequency aims to have both high penetration in human skin and tissues and high resolution. Indeed, low UWB frequencies tend to penetrate better than high frequencies. However, the latter offer advantages in terms of spatial resolution and antenna miniaturization, essential for our intended application. The receivers detect the reflected echoes, which carry modulations caused by respiration and heartbeat activity. These echoes are subsequently processed using advanced signal processing techniques to localize multiple targets and to estimate their respiratory and cardiac frequencies. The targets are modeled as inflection points at a distance d(t). Respiratory effects arise from thoracic and abdominal movements, with a breathing rate of 12 to 48 breaths per minute. Thoracic displacement amplitude varies between 4 mm to 12 mm, depending on the observer's position. Cardiac displacement, caused by heart contractions, ranges from 0.01 mm to several millimeters, with a heart rate of 60 to 120 beats per minute. The UWB signal propagation allows high-speed data transmission, but factors like attenuation, interference, and noise impact transmission quality. Gaussian white noise is simulated to model random interference, while attenuation reflects the signal strength loss during propagation, as illustrated in Figure 2.

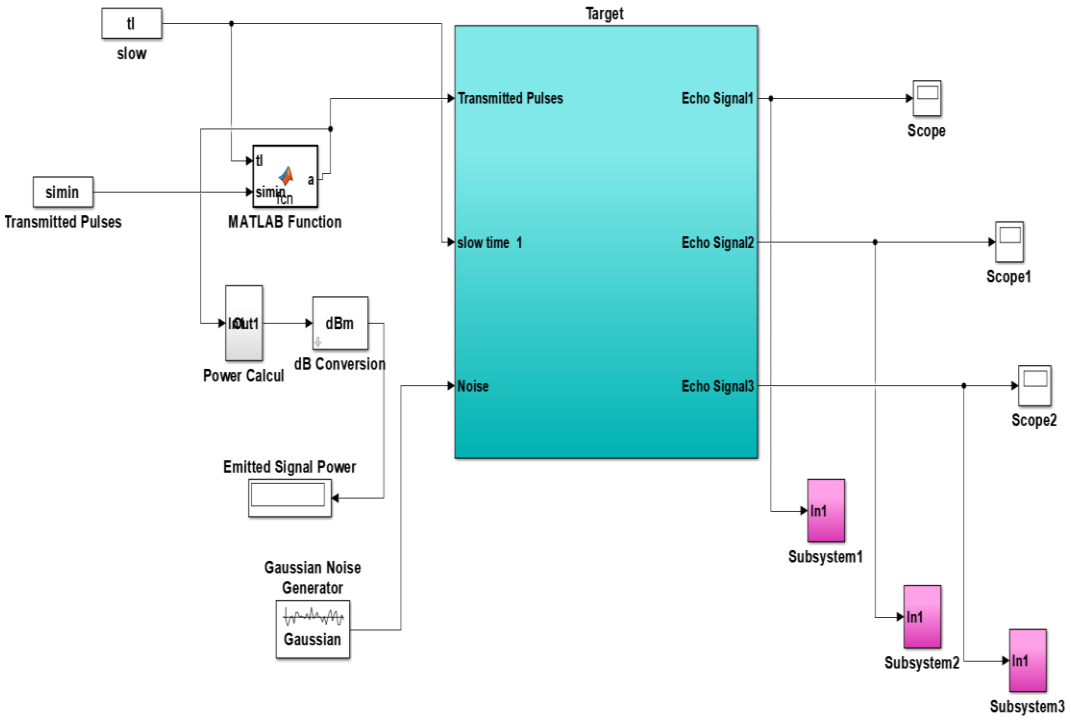

Figure 1. Proposed system

3.2.1. Data collection

The received waveforms are sampled at discrete points in slow time, the interval between successive acquisitions is $T_s = 0.02$ s, corresponding to a slow-time sampling frequency of $F_s = 50$ Hz. The total observation time is approximately 41 seconds, yielding 2,048 samples. For each waveform, the fast-time sampling frequency is set to $F_f = 50$ GHz, which results in a fast-time resolution of $T_f = 20$ ps.

The received signal is stored in a matrix R. For a discrete-time representation, the time indices are defined as $t = nT_s$ and $\tau = m\varepsilon_s$, leading to (6) [2]:

$$R_{N\times M} = r(nT_s, m\varepsilon_s) = \sum_{k=1}^{K} \alpha^k \, g\left(m\varepsilon_s - \tau^k(nT_s)\right) + \sum_i \alpha_i g(m\varepsilon_s - \tau_i) \quad (6)$$

ε_s represents the sampling interval in fast time, T_s represents the sampling interval in slow time. $m = 1,2,\ldots,M$, $n = 1,2,\ldots,N$ define the discrete indices in fast and slow time, respectively.

3.3. Signal pre-processing

Since the sensors operate as receivers, they will inevitably detect the echo from the transmitting sensor, as shown in Figure 3(a). Therefore, it is crucial to apply an effective filtering technique to suppress this echo and accurately extract the true signals reflected from the targets. To achieve this, the time mean subtraction (TMS) method is utilized as (7) and (8). Figure 3(b) shows the received signals after filtering.

$$\mu[m] = \frac{1}{N}\sum_{i=1}^{N} \tilde{R}[i,m] \quad (7)$$

$$\check{R}[n,m] = \tilde{R}[n,m] - \mu[m] \quad (8)$$

$\mu[m]$ denotes the mean value of the discretely received echo matrix $\tilde{R}[i,m]$.

Before suppression, the received signal is dominated by a strong component caused by transmitted signal leakage, as illustrated in Figure 3(a). This dominant component masks the reflections from the targets and degrades the accuracy of time-of-arrival (TOA) estimation.

After applying the suppression technique, the direct transmission component is effectively removed, allowing the target reflections to be clearly identified, as shown in Figure 3(b). Consequently, the performance of TOA extraction and distance estimation is significantly improved. The remaining peaks correspond to propagation delays, which are converted into range values, thereby enhancing the accuracy and reliability of TOA-based distance calculation and localization.

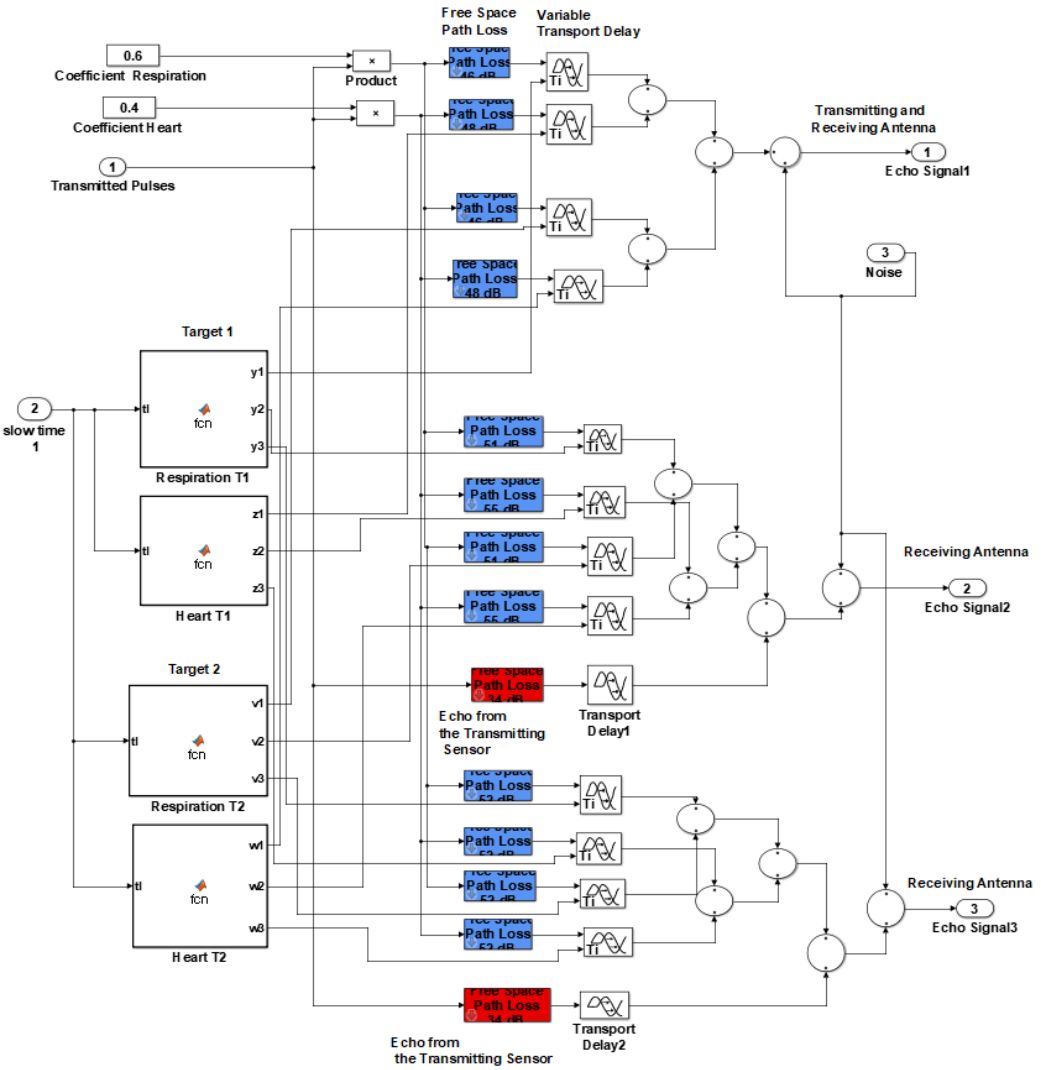

Figure 2. Proposed channel model

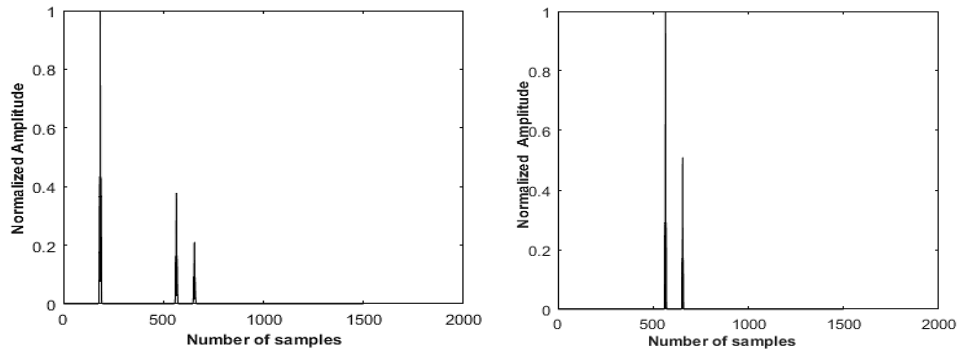

(a) (b)

Figure 3. Received signals from the receiving sensor; (a) before filtering and (b) after filtering

3.4. Localization multi-target

This section presents a method for localizing multiple targets using trilateration, which is based on measuring their distances from at least three sensor nodes. Each distance is represented as the radius of a circle centered at the corresponding sensor node and the target positions are determined from the intersections of these circles.

For an active sensor, the received signal yielded only a single peak when multiple targets were located at the same distance, making their separation challenging, as shown in Figure 4(a). To overcome this limitation, a network of sensors was employed. With three sensors, multiple targets could be localized and separated through triangulation, as each sensor provided an independent range measurement, as shown in Figure 4(b). Obviously, we can increase the number of sensors for more accuracy, but this in turn increases the computational complexity inherent in the GNN algorithm.

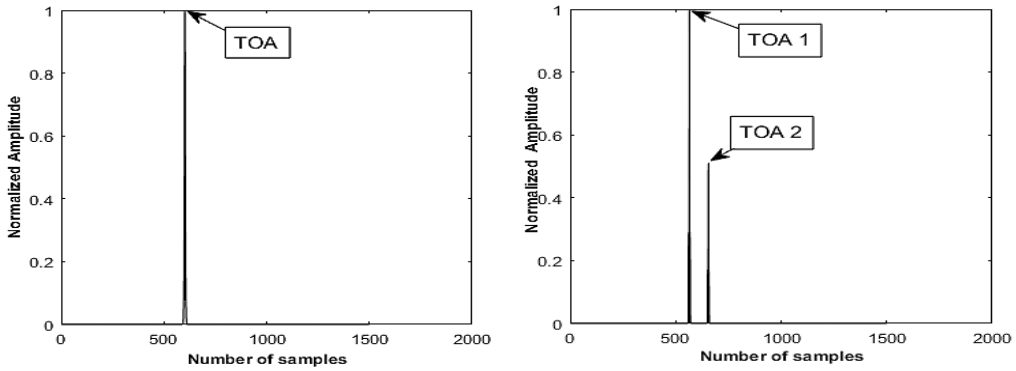

(a) (b)

Figure 4. Convoluted signal; (a) active sensor and (b) passive sensor

Since each sensor captures multiple TOA measurements, the main challenge lies in accurately associating each measurement with its corresponding target. The order of TOA values does not necessarily indicate the target's identity, as the closest target may differ across sensors. To resolve this ambiguity, a TOA association algorithm is employed to reliably map each detected TOA measurement to its respective target by systematically evaluating all possible peak–target assignment hypotheses, to accurately determine the true locations of the targets using combination of GNN and trilateration.
For a given target k ∈{1,2,…,K}and I sensors, the corresponding hypothesis set H_k is defined as:

$$H_k = \{(k, h_2, h_3, \dots, h_I): h_i \in \{1,2, \dots, K\}, \forall_i = 2, \dots, I\},$$

Where the peak k denotes the fixed TOA peak index at sensor S_1 associated with the target k, while the peaks at the other sensors vary to account for all possible TOA index assignments for sensors S_2 through S_I. The number of hypotheses for each target is given by:

$$H_k = K^{I-1} \tag{9}$$

The estimated TOAs are then converted into distances using the speed of light, as (10):

$$\check{d}_0^k = \frac{\check{\tau}^k * c}{2} \tag{10}$$

Where $\check{d}_0^k, \check{\tau}^k$ represent the estimated distance and the estimated TOA, respectively, between the active sensor and target k.
In contrast, for passive sensor, the distance is calculated as (11):

$$\check{d}_r^k = \frac{\check{\tau}_r^k}{c} - \check{d}_0^k \tag{11}$$

Where $\check{d}_r^k$ and $\check{\tau}_r^k$ represent the estimated distance and the estimated TOA, respectively, between the passive sensor and target k.

After estimating the distances, the trilateration technique was applied to determine the target positions. The GNN approach was then employed to evaluate all hypotheses by computing the Euclidean distance between the barycenter and the candidate locations, with the position yielding the minimum distance selected as the most probable.
Each radar i is positionned at (x_i, y_i), the possible locations of a target k as (12):

$$(x_k - x_i)^2 + (y_k - y_i)^2 = (\check{d}_i^k)^2 \tag{12}$$

(x_i, y_i) represents the known position of the radar i, (x_k, y_k) represents the unknown position of target k.

The equation simply states that the distance between the radar and the target is constant d_{ik}, any point (x, y) that satisfies this equation lies on a circle centered at (x_i, y_i) with radius $\check{d}_i^k$. For a target k, the distances expressed as (13)-(15):

$$(x_k - x_1)^2 + (y_k - y_1)^2 = (\check{d}_1^k)^2 \quad (13)$$

$$(x_k - x_2)^2 + (y_k - y_2)^2 = (\check{d}_2^k)^2 \quad (14)$$

$$(x_k - x_3)^2 + (y_k - y_3)^2 = (\check{d}_3^k)^2 \quad (15)$$

The equations are independent nonlinear simultaneous equations that cannot be solved mathematically. However, to address this problem, we use the intersection of circles. This is achieved by subtracting (13) from (14) and (13) from (15). The coordinates x and y can then be expressed as (16):

$$x_k = \frac{C_1 B_2 - C_2 B_1}{A_1 B_2 - A_2 B_1}, y_k = \frac{A_1 C_2 - A_2 C_1}{A_1 B_2 - A_2 B_1} \quad (16)$$

$$A_{1=}2(x_1 - x_2), B_{1=}2(y_1 - y_2), C_{1=}\left(x_1^2 + y_1^2 - d_{1j}^2\right) - (x_2^2 - y_2^2 - d_{2j}^2)$$

$$A_{2=}2(x_1 - x_3), B_{2=}2(y_1 - y_3), C_{2=}\left(x_1^2 + y_1^2 - d_{1j}^2\right) - (x_3^2 - y_3^2 - d_{3j}^2)$$

The barycenter of the intersection triangle is determined as the arithmetic mean of the coordinates of its vertices and is expressed as (17):

$$x_M = \frac{x_a + x_b + x_c}{3}, y_M = \frac{y_a + y_b + y_c}{3} \quad (17)$$

$(x_a, y_a), (x_b, y_b), (x_c, y_c)$ represent the coordinates of the intersection points.
Calculate the distances from points a, b, and c to point M, and identify the shortest distance.

$$d(a, M) = \sqrt{(x_a - x_M)^2 + (y_a - y_M)^2} \quad (18)$$

$$d(b, M) = \sqrt{(x_b - x_M)^2 + (y_b - y_M)^2} \quad (19)$$

$$d(c, M) = \sqrt{(x_c - x_M)^2 + (y_c - y_M)^2} \quad (20)$$

The principle of trilateration is used to determine the location of the target, as illustrated in Figure 5.

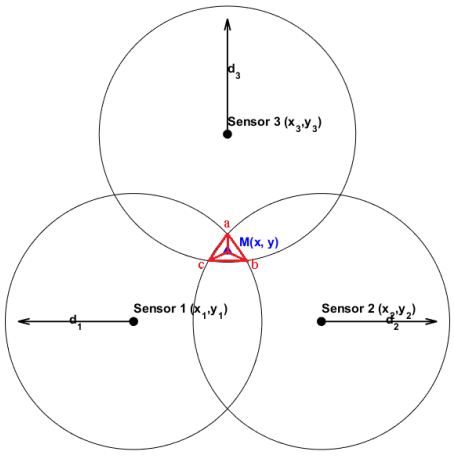

Figure 5. Principle of trilateration

3.5. Vital sign estimation

This work focuses on estimating the vital signs of each target based on its distance. After suppressing noise, the signal corresponding to each target can be defined as (21):

$$x(t,\tau) = \alpha\, g\big(\tau - \tau(t)\big) \tag{21}$$

Our goal is to estimate the breathing and heartbeat frequencies. To achieve this, the CTFT is applied along the slow-time axis [21].

$$X(f,\tau) = \int_{-\infty}^{+\infty} x(t,\tau) e^{-j2\pi f t}\, dt \tag{22}$$

$X(f,\tau)$ can be written as (23) [21], [22]:

$$X(f,\tau) = \alpha \sum_{n=-\infty}^{+\infty} \sum_{m=-\infty}^{+\infty} c_{nm}\ \delta(f - nf_b - mf_h) \tag{23}$$

δ denotes the Dirac function and c_{nm} is a coefficient that attains its maximum at $\tau = \tau_0$. It is evident that the spectrum is discrete, composed of a series of delta functions located at the harmonic frequencies of f_b, f_h [21], [22]. The breathing and heart rates were estimated by identifying the fundamental peaks within the frequency ranges of [0.2–0.8] Hz and [1–2] Hz, respectively.

4. EXPERIMENTAL RESULTS AND DISCUSSION

In this section, we describe the experiments conducted to assess the performance of the proposed method. The experiments aimed to estimate the location, breathing rate, and heart rate of two individuals based on simulated data. In the first experiment, the individuals were symmetrically positioned in front of the radar. The nominal distances from the transmitted radar were d_1=d_2=1.8 meters, as shown in Figure 6. For the first target, the respiratory rate was set at 0.27 Hz, and the heart rate was set at 1.2 Hz. For the second target, the respiratory rate was set at 0.32 Hz, and the heart rate was set at 1.5 Hz.

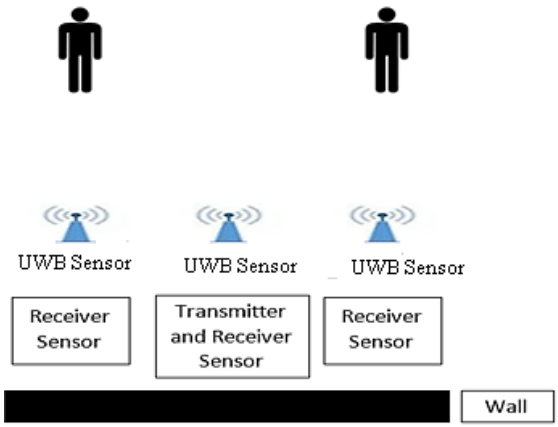

Figure 6. Experiment setup

In the second experiment, the individuals were positioned at different locations in front of the sensors, with nominal distances of d_1=1.4 meters and d_2=1.8 meters. For the first target, the respiratory rate was set at 0.29 Hz, and the heart rate was set at 1.6 Hz. For the second target, the respiratory rate was set at 0.35 Hz, and the heart rate was set at 1.8 Hz.

4.1. Position estimation

In this section, target localization is achieved using a combination of trilateration and GNN techniques. Due to the straight-line alignment of sensors, each hypothesis results in two possible locations, with one being unrealistic (the negative location) since it falls outside the feasible range. When two targets are equidistant from at least one sensor, the hypotheses remain identical. The goal is to accurately determine target locations by finding the common intersection of distance estimates from all sensors, which represents the most probable target position.

Figures 7 and 8 show the hypotheses for target locations in two experiments. In the first experiment, Hypothesis 1 and Hypothesis 4 correctly represent the positions of Target 1 (1.81 meters) and Target 2 (1.79 meters), with a 0.55% error. In the second experiment, Hypothesis 1 and Hypothesis 4 correctly represent Target 1 (1.42 meters, 1.42% error) and Target 2 (1.81 meters, 0.55% error).

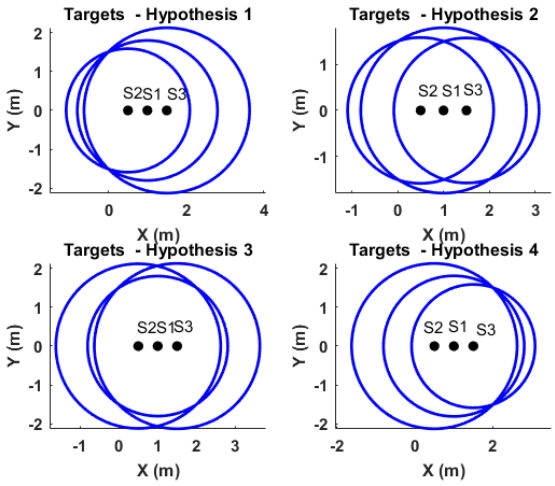

Figure 7. All hypotheses for both targets in the first experiment

In Experiment 1, subplots (1) and (4) in Figure 7 demonstrate that the trilateration method can reliably identify two distinct targets, as the intersections of the circles yield two consistent solutions corresponding to the actual target positions. In Experiment 2, subplot Figure 8(a) corresponds to the first target, while subplot Figure 8(b) represents the second target, both illustrating accurate localization. These results validate the effectiveness of trilateration in reliably localizing and separating multiple targets within the sensing area. The estimated positions make it possible to separate the targets' signals based on their corresponding distances.

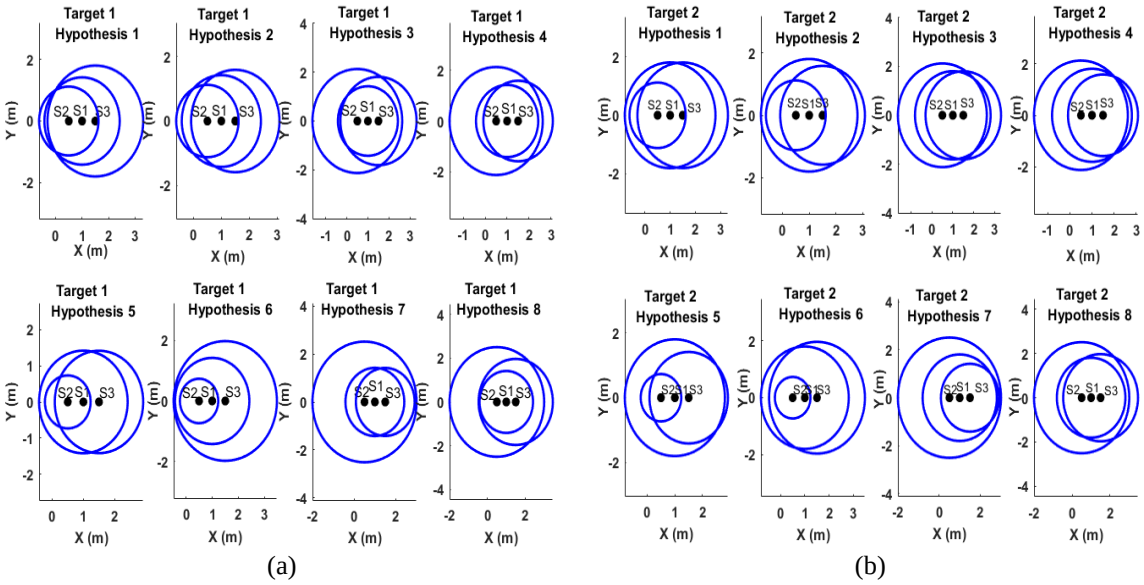

(a) (b)

Figure 8. All hypotheses in the second experiment; (a) Target 1 and (b) Target 2

4.2. Vital signs estimation

In this section, the vital sign rates are estimated using the CTFT, where the separation of signals is achieved based on the estimated distances. The breathing rate corresponds to the fundamental peak within the range of [0.2, 0.8] Hz, while the heart rate is identified by the peak within the range of [1, 2] Hz. In the first experiment, for the first target, the breathing rate was estimated to be 0.2686 Hz with a relative error of 0.52%, whereas the heart rate was estimated to be 1.196 Hz, with a relative error of 0.34%, as shown in Figure 9(a).

For the second target, the breathing rate was estimated to be 0.3174 Hz, with a relative error of 0.81%, while the heart rate was estimated to be 1.489 Hz, with a relative error of 0.73%, as shown in Figure 9(b). In the

second experiment, the breathing rate for the first target was estimated to be 0.293 Hz with a relative error of 1%, while the heart rate was estimated to be 1.611 Hz, with a relative error of 0.69% as shown in Figure 10(a). For the second target, the breathing rate was estimated to be 0.3418 Hz, with a relative error of 2.34%, while the heart rate was estimated to be 1.807 Hz, with a relative error of 0.39%, as shown in Figure 10(b).

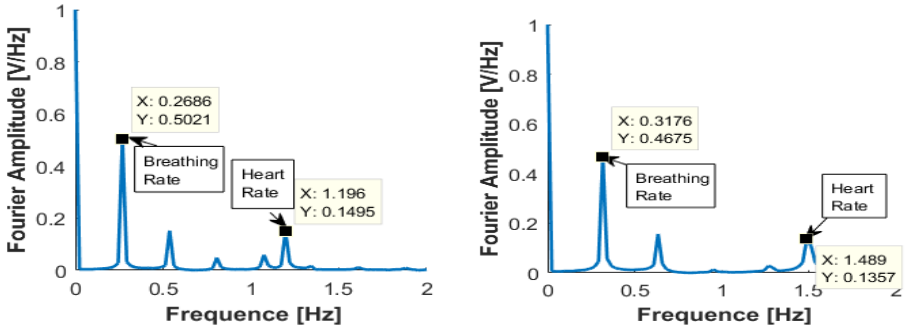

(a) (b)

Figure 9. Breathing rate and heart rate for two persons in the first experiment; (a) Target 1 and (b) Target 2

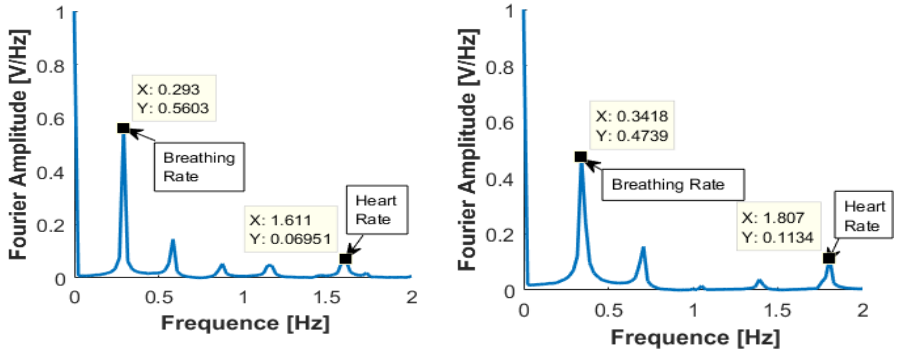

(a) (b)

Figure 10. Breathing rate and heart rate for two persons in the second experiment; (a) Target 1 and (b) Target 2

4.2.1. Comparison

Compared to existing methods, the proposed method offers higher localization accuracy and yields lower estimation errors in both respiration rate and heart rate, as shown in Table 1.

Table 1. Comparison with the state-of-the-art research

Research paper	Localization algorithm	Vital signs algorithm	Distance estimation error	Respiration rate error (%)	Heart rate error (%)
[2]	Permutation entropy and K means++ clustering	EEMD-WA	1.83%	4.27	6.23
[24]	Improved high-precision multi-signal classification (IHAMUSIC)	Variational modal decomposition technique based on the sparrow search algorithm (SSA-VMD)	None	3.98	4.57
[25]	None	Template matching estimation (TME) and multi-range bins timing eigenvalues using neural network	None	9.42	9.75
This paper	**Association TOA and trilateration**	**CTFT**	**1.42%**	**2.34**	**0.73**

5. CONCLUSION

In this study, we proposed a non-contact solution for localizing and monitoring multiple individuals located at same distance. As a preprocessing step, we applied the TMS method to suppress signals originating from the transmitting sensor, followed by analyzing all possible TOA hypotheses to accurately determine the true locations of the targets using combination of Trilateration and GNN. Additionally, we employed the

CTFT to extract both respiration and heart rates. The experimental results demonstrated that the proposed system effectively localized multiple individuals while accurately estimating their breathing and heart rates. Future work may integrate machine learning for improved TOA prediction and adaptive thresholding to enhance robustness in noisy environments.

FUNDING INFORMATION

Authors state no funding involved.

AUTHOR CONTRIBUTIONS STATEMENT

This journal uses the Contributor Roles Taxonomy (CRediT) to recognize individual author contributions, reduce authorship disputes, and facilitate collaboration.

Name of Author	C	M	So	Va	Fo	I	R	D	O	E	Vi	Su	P	Fu
Meraouli Hadjer Rania	✓	✓	✓			✓			✓	✓				
Slimane Zohra		✓	✓			✓	✓		✓			✓		
Abdelmalek Abdelhafid	✓		✓	✓	✓					✓				

C : **C**onceptualization
M : **M**ethodology
So : **So**ftware
Va : **Va**lidation
Fo : **Fo**rmal analysis
I : **I**nvestigation
R : **R**esources
D : **D**ata Curation
O : Writing - **O**riginal Draft
E : Writing - Review & **E**diting
Vi : **Vi**sualization
Su : **Su**pervision
P : **P**roject administration
Fu : **Fu**nding acquisition

CONFLICT OF INTEREST STATEMENT

Authors state no conflict of interest.

DATA AVAILABILITY

Data availability is not applicable to this paper as no new data were created or analyzed in this study.

REFERENCES

[1] I. Kakouche, H. Abadlia, M. N. El Korso, A. Mesloub, A. Maali, and M. S. Azzaz, "Joint vital signs and position estimation of multiple persons using simo radar," *Electronics*, vol. 10, no. 22, pp. 1–15, 2021, doi: 10.3390/electronics10222805.

[2] J. Zhang *et al.*, "A Multi-Target Localization and Vital Sign Detection Method Using Ultra-Wide Band Radar," *Sensors*, vol. 23, no. 13, p. 5779, 2023, doi: 10.3390/s23135779.

[3] A. Sarkar and D. Ghosh, "Accurate sensing of multiple humans buried under rubble using IR-UWB SISO radar during search and rescue," *Sensors and Actuators A: Physical*, vol. 348, pp. 1–10, 2022, doi: 10.1016/j.sna.2022.113975.

[4] C. Shi, Z. Zheng, J. Pan, Z. K. Ni, S. Ye, and G. Fang, "Multiple Stationary Human Targets Detection in Through-Wall UWB Radar Based on Convolutional Neural Network," *Applied Sciences*, vol. 12, no. 9, 2022, doi: 10.3390/app12094720.

[5] Y. Zhang *et al.*, "A coarse-to-fine detection and localization method for multiple human subjects under through-wall condition using a new telescopic SIMO UWB radar," *Sensors and Actuators A: Physical*, vol. 332, p. 113064, 2021, doi: 10.1016/j.sna.2021.113064.

[6] J. Xiong, H. Hong, H. Zhang, N. Wang, H. Chu, and X. Zhu, "Multitarget respiration detection with adaptive digital beamforming technique based on simo radar," *IEEE Transactions on Microwave Theory and Techniques*, vol. 68, no. 11, pp. 4814–4824, 2020, doi: 10.1109/TMTT.2020.3020082.

[7] J. Pan *et al.*, "A Multi-Target Detection Method Based on Improved U-Net for UWB MIMO Through-Wall Radar," *Remote Sens.*, vol. 15, no. 13, 2023, doi: 10.3390/rs15133434.

[8] C. Feng *et al.*, "Multitarget Vital Signs Measurement with Chest Motion Imaging Based on MIMO Radar," *IEEE Transactions on Microwave Theory and Techniques*, vol. 69, no. 11, pp. 4735–4747, 2021, doi: 10.1109/TMTT.2021.3076239.

[9] Z. Li, T. Jin, Y. Dai, and Y. Song, "Through-wall multi-subject localization and vital signs monitoring using uwb mimo imaging radar," *Remote Sensing*, vol. 13, no. 15, pp. 1–21, 2021, doi: 10.3390/rs13152905.

[10] A. T. Kristensen, S. Li, A. Balatsoukas-Stimming, and A. Burg, "Monostatic Multi-Target Wi-Fi-Based Breathing Rate Sensing Using Openwifi," in *2024 IEEE Wireless Communications and Networking Conference (WCNC)*, Dubai, United Arab Emirates, 2024, pp. 1–6, doi: 10.1109/WCNC57260.2024.10570912.

[11] A. Shokouhmand, S. Eckstrom, B. Gholami and N. Tavassolian, "Camera-Augmented Non-Contact Vital Sign Monitoring in Real Time," in *IEEE Sensors Journal*, vol. 22, no. 12, pp. 11965-11978, Jun. 2022, doi: 10.1109/JSEN.2022.3172559.

[12] S. M. M. Islam, O. Boric-Lubecke, and V. M. Lubekce, "Concurrent Respiration Monitoring of Multiple Subjects by Phase-Comparison Monopulse Radar Using Independent Component Analysis (ICA) with JADE Algorithm and Direction of Arrival

(DOA)," *IEEE Access*, vol. 8, pp. 73558–73569, 2020, doi: 10.1109/ACCESS.2020.2988038.
[13] M. Nosrati, S. Shahsavari, S. Lee, H. Wang, and N. Tavassolian, "A Concurrent Dual-Beam Phased-Array Doppler Radar Using MIMO Beamforming Techniques for Short-Range Vital-Signs Monitoring," in *IEEE Transactions on Antennas and Propagation*, vol. 67, no. 4, pp. 2390-2404, Apr. 2019, doi: 10.1109/TAP.2019.2893337.
[14] Y. Yuan and C. T. M. Wu, "Recent development of non-contact multi-target vital sign detection and location tracking based on metamaterial leaky wave antennas," *Sensors*, vol. 21, no. 11, pp. 1-21, 2021, doi: 10.3390/s21113619.
[15] C. Ding, J. Yan, L. Zhang, H. Zhao, H. Hong, and X. Zhu, "Noncontact multiple targets vital sign detection based on VMD algorithm," in *2017 IEEE Radar Conference (RadarConf)*, Seattle, WA, USA, 2017, pp. 0727-0730, doi: 10.1109/RADAR.2017.7944298.
[16] Z. Liang, Y. Jin, D. Yang, B. Liang, and J. Mo, "Two-Step Accuracy Improvement for Multitarget Detection in Complex Environment Using UWB Radar," *Remote Sensing*, vol. 16, no. 5, pp. 1–19, 2024, doi: 10.3390/rs16050877.
[17] X. Shang, J. Liu, and J. Li, "Multiple Object Localization and Vital Sign Monitoring Using IR-UWB MIMO Radar," in *IEEE Transactions on Aerospace and Electronic Systems*, vol. 56, no. 6, pp. 4437-4450, Dec. 2020, doi: 10.1109/TAES.2020.2990817.
[18] A. Rittiplang and P. Phasukkit, "UWB Radar for Multiple Human Detection Through the Wall Based on Doppler Frequency and Variance Statistic," in *2019 12th Biomedical Engineering International Conference (BMEiCON)*, Ubon Ratchathani, Thailand, 2019, pp. 1-5, doi: 10.1109/BMEiCON47515.2019.8990358.
[19] Q. Deng, J. Le, S. Barbat, R. Tian and Y. Chen, "Efficient living subject localization and weak vital-sign signal enhancement using impulse radio based UWB radar," in *2019 IEEE Intelligent Vehicles Symposium (IV)*, Paris, France, 2019, pp. 777-782, doi: 10.1109/IVS.2019.8814004.
[20] M. Dou and W. Zhang, "Improved ranging method for life detection using ultra-wide band impulse radar," *The Journal of Engineering*, vol. 2018, no. 10, pp. 1375–1383, 2018, doi: 10.1049/joe.2018.5023.
[21] Z. Slimane and A. Abdelhafid, "Through Wall Stationary Human Target Detection and Localization Using OFDM-UWB Radar," *Frequenz*, vol. 70, no. 5–6, pp. 245–251, 2016, doi: 10.1515/freq-2015-0156.
[22] A. Lazaro, D. Girbau, and R. Villarino, "Analysis of vital signs monitoring using an IR-UWB radar," *Progress In Electromagnetics Research*, vol. 100, pp. 265–284, 2010, doi: 10.2528/PIER09120302.
[23] J. C. Mcmi and S. S. Lim, "Data Association Algorithms for Multiple Target Tracking (U)," *Def. Res. Establ. Ottawa*, 1990.
[24] Z. Huo, Z. Zhang, Y. Yin, H. Chen, and Z. Shen, "Research on Multitarget Vital Sign Detection Using IR-UWB Radar in Occlusion Scenarios," in *IEEE Sensors Journal*, vol. 24, no. 9, pp. 15327-15336, May 2024, doi: 10.1109/JSEN.2024.3380831.
[25] E.-K. Wu *et al*., "Non-contact monitoring of human cardiorespiratory activity during sleep using FMCW millimeter wave radar," *Measurement*, vol. 242, p. 116144, 2025, doi: 10.1016/j.measurement.2024.116144.

BIOGRAPHIES OF AUTHORS

Meraouli Hadjer Rania obtained Master's degree in Network and Telecommunication from the University of Sidi Bel Abbes, Algeria, in 2020. She is currently pursuing a Ph.D. in Network and Telecommunication at the University of Ain Temouchent, where she is also affiliated with the Structures Intelligentes Laboratory (SSL). Her research interests lie in the area of healthcare systems and technologies involving ultra wide band sensors, signal processing, remote monitoring, embedded systems, machine learning, data privacy, and security. She can be contacted at email: hadjer.meraouli@univ-temouchent.edu.dz or hadjermeraouli@gmail.com.

Slimane Zohra received Magister Diploma (2008), Ph.D. (2012) and HDR (2017), in Telecommunication from Tlemcen University (Algeria). Since 2008, she has been researcher at STIC Laboratory and system engineer at Sonatrach Aval Research Group. In 2014, she joined Belhadj Bouchaib University Center (Algeria), where she worked as associate and research Professor, responsible for LMD graduation and doctorate training in the telecommunications sector. In 2022, she joined Tlemcen University (Algeria). Since 2019, she has been involved as project leader dedicated to indoor localization. Her research interests include location and imaging radars, UWB sensors, networking, mobile networks, ubiquitous internet, and next-generation networks. She can be contacted at email: zohra.slimane@univ-tlemcen.dz or zoh_slimani@yahoo.fr.

Abdelmalek Abdelhafid received the Laurea degree in Telecommunication Engineering from Institute of Telecommunications Oran (Algeria) in 1991, and Diploma of deepened studies in optoelectronic at Nancy (France) in 1993. From 1994 to 2000, he worked as engineer in charge of design and management of ISDN networks at Algerie Telecoms Company. In 2002, he received Magister Diploma in Signals and systems at Tlemcen University, Algeria. He subsequently joined the faculty of technology and STIC Laboratory as research Professor. He received the Ph.D. degree in Electronics in 2013. He has participated in several national research frameworks and projects. His main research activities cover radar, data communications, mobile networks, security, protocols and high-speed optical networks. He can be contacted at email: abdelmalekabdelhafid@gmail.com.